University of Science and Technology Houari Boumediene (USTHB)
Faculty of Mechanical Engineering and Process Engineering
Department of Mechanical Design and Manufacturing

Analysis and Simulation of Human–Lower-Limb Exoskeleton Interaction for Pediatric Gait in Cerebral Palsy

Summary of Final Year Engineering Project (PFE)

Academic Year 2025–2026

Presented by: BOUDJEDIR Sara KENDEL Rabab
Supervisor: Pr. BELOUCHRANI M.A. (CMP-USTHB)
Co-supervisor: Mr. ZENNADI K. (ENP)
Institution: University of Science and Technology Houari Boumediene (USTHB)
Degree: Master's Degree in Mechanical Engineering
Specialization: Mechanical Design
Academic Year: 2025–2026
Keywords: Lower-limb exoskeleton, Cerebral palsy, Biomechanical modeling, Deep learning, Synthetic gait data, CNN-BiLSTM, Torque prediction

Abstract

This thesis presents a unified framework combining physics-based biomechanical modeling and deep learning to support the design of pediatric lower-limb exoskeletons. An eight-degree-of-freedom sagittal-plane model is formulated using the Denavit–Hartenberg convention and Lagrangian dynamics. Since clinical datasets for children with cerebral palsy (CP) are scarce, a synthetic pathological-gait database is generated through controlled perturbations of healthy gait trials. A CNN–BiLSTM network then learns to predict the joint torque corrections required at the hip and knee from kinematic inputs alone. The biomechanical model achieves correlation coefficients of 0.69–0.91 against Plug-in Gait reference moments; the neural network reaches $R^2 = 0.90$–0.91 on synthetic data and produces physically consistent corrections on real clinical recordings. Preliminary actuator sizing estimates up to $\approx 13\,\mathrm{N{\cdot}m}$ are derived for hip and knee joints.

Contents

List of Abbreviations

Abbreviation	Definition
BiLSTM	Bidirectional Long Short-Term Memory
CNN	Convolutional Neural Network
CoM	Center of Mass
CoP	Center of Pressure
CP	Cerebral Palsy
DH	Denavit–Hartenberg (kinematic convention)
DOF	Degree(s) of Freedom
ENP	École Nationale Polytechnique d'Alger
FC	Fully Connected (layer)
GMFCS	Gross Motor Function Classification System
GRF	Ground Reaction Force
HJC	Hip Joint Center
IC	Initial Contact (gait event)
KJC	Knee Joint Center
AJC	Ankle Joint Center
LSTM	Long Short-Term Memory
MAE	Mean Absolute Error
MSE	Mean Squared Error
PFE	Projet de Fin d'Études (Final Year Engineering Project)
PiG	Plug-in Gait (Vicon inverse-dynamics model)
ReLU	Rectified Linear Unit
RMSE	Root Mean Square Error
SMA	Spinal Muscular Atrophy
TD	Typically Developing (healthy reference child)

Introduction and Motivation

Walking is one of the most fundamental human activities, yet neurological disorders can severely impair it. **Cerebral palsy (CP)** is the leading cause of motor disability in children, affecting approximately 2–3 per 1 000 live births. The disorder originates from non-progressive lesions of the developing brain and manifests through spasticity, muscular weakness, and impaired neuromuscular control, ultimately producing characteristic gait deviations at the ankle (equinus, varus), knee (crouch, stiff-knee), and hip (excessive flexion, adduction).

Lower-limb exoskeletons have emerged as promising rehabilitation devices that can assist walking, reduce therapist burden, and enable intensive gait training outside clinical settings. However, designing such systems for children presents unique engineering challenges:

- Children's bodies grow continuously, demanding adaptable mechatronics.
- Pediatric gait databases are scarce due to ethical and logistical constraints on clinical studies.
- Assistance profiles must be individualized to each child's specific pathological pattern rather than fixed to a single average template.

Central Research Question

How can we estimate the joint torques required to assist a child with cerebral palsy during walking, while minimizing the dependence on extensive clinical datasets that are difficult to collect ethically?

This work answers this question by coupling a **validated physics-based model** with a **data-driven neural network**, where the physics model generates the synthetic data that the neural network requires for training. The two approaches thus complement each other rather than compete.

Chapter I – Lower-Limb Exoskeletons and Pediatric Systems

Overall Methodological Framework

Before diving into each chapter, the figure below summarizes the overall pipeline that structures the entire project.

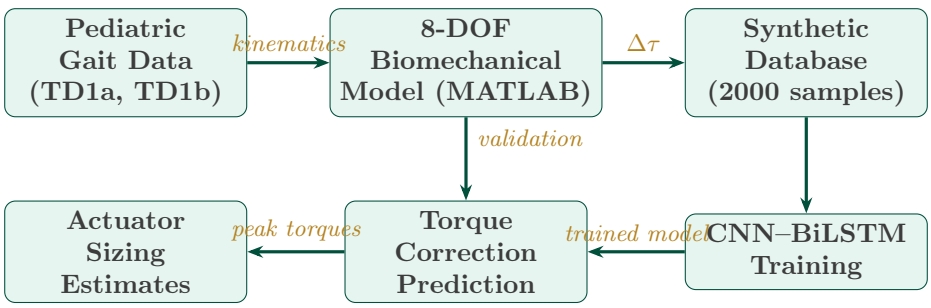

Definition and Classification

An exoskeleton is a wearable robotic structure that wraps around the user's limb segments and applies torques or forces at the biological joints. Lower-limb exoskeletons are classified by

their target population (adult / pediatric), application (rehabilitation / mobility assistance), and actuation strategy (active / passive / quasi-passive).

Active exoskeletons use motorized joints driven by a control law; passive devices store and release energy through springs or dampers; quasi-passive devices add small actuation on a predominantly passive mechanism. This project focuses on **active** assistance, where computed torque profiles directly drive the actuators.

Evolution and State of the Art

Interest in powered lower-limb exoskeletons grew substantially in the 2000s. For adult rehabilitation, commercially available systems include the **Lokomat** (Hocoma), the **Walkbot** (P&S Robotics), and the **HAL** (Cyberdyne). For pediatric users specifically, the landscape is much more limited:

System	Developer	Key Feature
ATLAS 2030	Marsi Bionics (Spain)	Fully active, 6 DoF per leg; clinical trials in SMA and CP children
CPWalker	CSIC (Spain)	Overground rehabilitation robot for CP
Trexo Plus	Trexo Robotics (CA)	Wheelchair-mountable, compatible from age 2
ExoAtlet Bambini	ExoAtlet (RU)	Pediatric version of adult platform
H-MEX	Hyundai (KR)	Adjustable segments for growing users

Cerebral Palsy: Epidemiology and Clinical Context

Cerebral palsy is an umbrella term for a group of permanent, but non-progressive, disorders of movement and posture resulting from disturbances that occurred in the developing fetal or infant brain. Key epidemiological and clinical facts relevant to this project:

- Prevalence: 2–3 per 1 000 live births; estimated 17 million people worldwide.
- The gait impairment results from **upper motor neuron lesions**, causing spasticity, co-contraction, and loss of selective motor control – but the musculoskeletal structure itself is initially intact, unlike neuromuscular diseases.
- For this reason, **joint-level modeling is the appropriate entry point**: assisting the joints directly compensates for the neural deficit without requiring explicit neuromuscular simulation.
- The GMFCS classifies functional severity into five levels; exoskeleton assistance is most relevant for Levels II–IV.

Human–Exoskeleton Interaction

The coupled system (human + device) is modeled as two structures sharing the same joint axes. Under the rigid-coupling assumption, each joint has a single generalized coordinate, and the inertial properties are additive. This simplification is standard in the literature and is adopted throughout this work. The primary design challenge lies in ensuring that the exoskeleton torques assist the human without inducing parasitic forces at the attachment interfaces.

Chapter II – Biomechanics of Human Gait and Cerebral Palsy

Reference Gait Data

The healthy reference data used throughout this work come from a **publicly available pediatric gait database** containing three-dimensional motion-capture recordings of typically developing (TD) children. Two trials were selected:

- **TD1a** and **TD1b**: two recordings of the same healthy child walking at self-selected speed. Each trial provides synchronized joint angles (from inverse kinematics), joint moments (from the Plug-in Gait inverse-dynamics model), ground reaction forces (from force plates), and pelvis translations – all at a sampling rate of 100 Hz.

For the pathological validation, two cerebral-palsy trials are used:

- **DiCP2**: mild-to-moderate diplegia.
- **DiCP3a**: more severe diplegia, showing pronounced crouch gait at the knee and excessive hip flexion.

These clinical trials are used *exclusively for evaluation*; they are never seen by the neural network during training.

Normal Gait

A **gait cycle** begins when one foot contacts the ground (initial contact) and ends when the same foot contacts the ground again. It is divided into:

- **Stance phase** ($\approx 60\%$): the foot is in contact with the ground; the body's weight is transferred, supported, and propelled.
- **Swing phase** ($\approx 40\%$): the foot is airborne; the limb advances to the next step.

Normal gait is a highly energy-efficient process. The center of mass follows a sinusoidal trajectory minimizing vertical displacement; tendon elastic recoil contributes to propulsion; and foot rockers (heel, ankle, forefoot) convert the vertical fall of the body into forward progression. Sagittal-plane joint angles during normal gait are well characterized: the hip flexes $\approx 30^\circ$ at initial contact and extends to $\approx 10^\circ$ at push-off; the knee peaks at $\approx 60^\circ$ during swing; the ankle dorsiflexes $\approx 15^\circ$ during mid-stance before rapid plantarflexion at push-off.

Normal Gait – Key Kinematic Values

The following table summarizes the key sagittal-plane joint angle ranges during normal walking, which serve as the *healthy reference* that CP deviations are measured against:

Joint	Range of motion	Peak (phase)	Function
Hip flex/ext	$\approx 40^\circ$	30° flex (IC)	Weight acceptance, propulsion
Knee flex/ext	$\approx 60^\circ$	60° flex (swing)	Foot clearance, shock absorption
Ankle DF/PF	$\approx 30^\circ$	15° DF (mid-stance); 20° PF (push-off)	Propulsion, controlled descent

IC = initial contact; DF = dorsiflexion; PF = plantarflexion.

These ranges define the **healthy trajectory corridor** that the neural network learns as its baseline. Any deviation from these profiles, as parameterized by the synthetic perturbations, defines the required assistance torque correction.

Pathological Gait in Cerebral Palsy

CP disrupts gait through **spasticity** (velocity-dependent hypertonia) and **impaired neural control**. Winter's classification identifies characteristic kinetic control errors rather than purely kinematic descriptions:

Joint	Deviation	Underlying Cause
Ankle	Equinus (plantarflexion throughout)	Gastrocnemius spasticity
	Varus (inversion)	Tibialis anterior imbalance
Knee	Crouch gait (excessive flexion)	Hamstring spasticity
	Stiff-knee gait (reduced swing flex.)	Rectus femoris spasticity
Hip	Excessive flexion, adduction	Hip flexor and adductor spasticity

The **Gross Motor Function Classification System (GMFCS)** grades CP severity from Level I (walks without restrictions) to Level V (severely limited self-mobility). This classification is used in this work to parameterize the severity of synthetic gait perturbations.

Chapter III – Mathematical Modeling of the Biomechanical System

Schematic of the 8-DOF Model

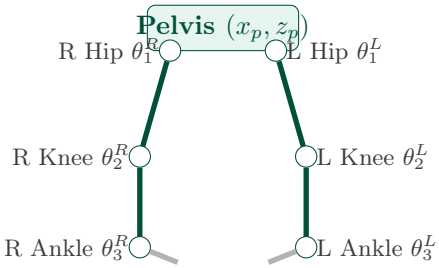

8 DOF total: 2 unactuated (pelvis translation) + 6 actuated (joints)

System Architecture: 8-DOF Floating-Base Model

The lower-limb system is modeled as **two planar kinematic chains (legs) attached to a common floating pelvis**. The generalized-coordinate vector is:

$$\mathbf{q} = \left[x_p,\ z_p,\ \theta^R_{\text{hip}},\ \theta^R_{\text{knee}},\ \theta^R_{\text{ankle}},\ \theta^L_{\text{hip}},\ \theta^L_{\text{knee}},\ \theta^L_{\text{ankle}}\right]^\top \in \mathbb{R}^8$$

where (x_p, z_p) are the pelvis translations in the sagittal plane (2 unactuated DOF) and the remaining six angles are the actuated joint coordinates. The **floating base** is essential: a fixed-base assumption would produce artificial reaction torques at the pelvis that do not correspond to physical reality.

Why a Floating Base?

Fixing the pelvis to the ground is a common simplification but forces the model to generate non-physical "ground reaction" torques at the pelvis. A floating base allows the pelvis to move freely and projects the true ground reaction forces (GRFs) at the foot via the Jacobian, giving physically consistent joint torque estimates during stance.

Denavit–Hartenberg Kinematics

The kinematic chain of each leg is described using the **Denavit–Hartenberg (DH) convention**. For a planar leg (all joint axes perpendicular to the sagittal plane), the twist α_{i-1} and offset r_i are zero for every joint, leaving only the joint angle θ_i and the preceding link length d_{i-1} as active parameters:

Joint i	Segment	α_{i-1}	d_{i-1}	θ_i	r_i
1	Hip	0	0	θ_1	0
2	Knee	0	l_1	θ_2	0
3	Ankle	0	l_2	θ_3	0

where l_1 (thigh) and l_2 (shank) are the segment lengths derived from pediatric anthropometric scaling (Winter 2009, child $H = 1.30\,\text{m}$, $M = 30\,\text{kg}$).

Pediatric Anthropometric Parameters

The mass matrix M, Coriolis vector C, and gravity vector G all depend on the physical properties of each body segment. These are estimated via Winter's (2009) proportional scaling laws for a reference child ($H = 1.30\,\text{m}$, $M = 30\,\text{kg}$):

Segment	**Length l (m)**	**Mass m (kg)**	**CoM fraction**	**I (kg·m^2)**
Thigh	0.2925	3.570	0.433	0.065
Shank	0.2717	1.470	0.433	0.021
Foot	0.1170	0.420	0.500	0.002

Parameters for both legs (R and L) are assumed symmetric. The vector of 27 parameters $\mathbf{p}$ groups lengths, masses, CoM fractions, moments of inertia, and two joint offsets (hip, ankle) required for the DH frame alignment.

Lagrangian Dynamics

The equations of motion are derived via the Euler–Lagrange formulation implemented **symbolically in MATLAB** using the Symbolic Math Toolbox:

$$\boxed{M(\mathbf{q})\,\ddot{\mathbf{q}} + C(\mathbf{q},\dot{\mathbf{q}})\,\dot{\mathbf{q}} + G(\mathbf{q}) = \boldsymbol{\tau} + \mathbf{J}_{\text{CoP}}^{\top}\,\mathbf{F}_{\text{GRF}}}$$

- $M(\mathbf{q})$: symmetric positive-definite mass matrix
- $C(\mathbf{q},\dot{\mathbf{q}})\dot{\mathbf{q}}$: Coriolis and centrifugal vector
- $G(\mathbf{q})$: gravity vector
- $\boldsymbol{\tau}$: generalized joint torques (control inputs)
- $\mathbf{J}_{\text{CoP}}^{\top}\mathbf{F}_{\text{GRF}}$: ground reaction forces projected via the center-of-pressure Jacobian

Symbolic derivation generates optimized numerical functions `M_func.m`, `Cqdot_func.m`, and `G_func.m`, making the model computationally efficient for repeated evaluation across thousands of gait frames.

Forward Kinematics

Given the joint angles $\mathbf{q}$, the position of each joint center and segment CoM is computed by composing the DH transforms. For the right leg, the joint centers are:

$$\mathbf{p}_{\text{HJC}} = \begin{bmatrix} x_p \\ z_p \end{bmatrix}, \quad \mathbf{p}_{\text{KJC}} = \mathbf{p}_{\text{HJC}} + l_1 \begin{bmatrix} \sin\phi_1 \\ -\cos\phi_1 \end{bmatrix}, \quad \mathbf{p}_{\text{AJC}} = \mathbf{p}_{\text{KJC}} + l_2 \begin{bmatrix} \sin\phi_2 \\ -\cos\phi_2 \end{bmatrix}$$

where $\phi_1 = \theta_{\text{hip}} + \delta_{\text{hip}}$ and $\phi_2 = \phi_1 - \theta_{\text{knee}}$ are the absolute segment angles in the global frame, and $\delta_{\text{hip}}, \delta_{\text{ankle}}$ are fixed anatomical offset angles. This parameterization avoids gimbal-lock issues and is consistent with the Plug-in Gait convention.

The **velocity Jacobian $\mathbf{J}_k$** mapping joint velocities to the linear velocity of each point is obtained by differentiating the position vector with respect to $\mathbf{q}$. These Jacobians are used both for the Coriolis terms and for projecting ground reaction forces into joint torques during the stance phase.

MATLAB Symbolic Implementation

A key engineering contribution of this work is the use of the **MATLAB Symbolic Math Toolbox** to derive all dynamic quantities analytically. The workflow is:

1. Define all system parameters (l, m, c, I) as symbolic variables.
2. Compute kinetic energy T and potential energy V symbolically.
3. Apply the Euler–Lagrange operator to obtain $\boldsymbol{\tau}$.
4. Factor out M, $C\dot{\mathbf{q}}$, and G algebraically via Jacobians with respect to $\ddot{\mathbf{q}}$ and $\dot{\mathbf{q}}$.
5. Export optimized numerical functions (`M_func.m`, `Cqdot_func.m`, `G_func.m`) via `matlabFunction()`.

This symbolic-then-numerical strategy ensures **exact derivatives** (no finite-difference approximation errors) while remaining efficient enough to evaluate over thousands of frames in milliseconds per frame.

Model Validation

The model is validated in **swing phase** against reference joint moments from the Plug-in Gait (PiG) inverse-dynamics pipeline, using two healthy pediatric trials (TD1a, TD1b). The comparison is restricted to the swing phase because the current model does not yet incorporate GRFs.

Validation Results – Dynamic Model (Swing Phase)

Joint	Correlation r	R^2	Agreement
R Hip	0.69	0.42	Moderate
R Knee	0.68	–	Weak (amplitude underestimation)
R Ankle	0.89	0.79	Strong
L Hip	0.87	0.75	Strong
L Knee	0.87	0.76	Strong
L Ankle	0.91	0.81	Strong

5 of 6 joints show moderate-to-strong agreement. The right knee amplitude underestimation is attributed to anthropometric uncertainties and is reflected in the training data.

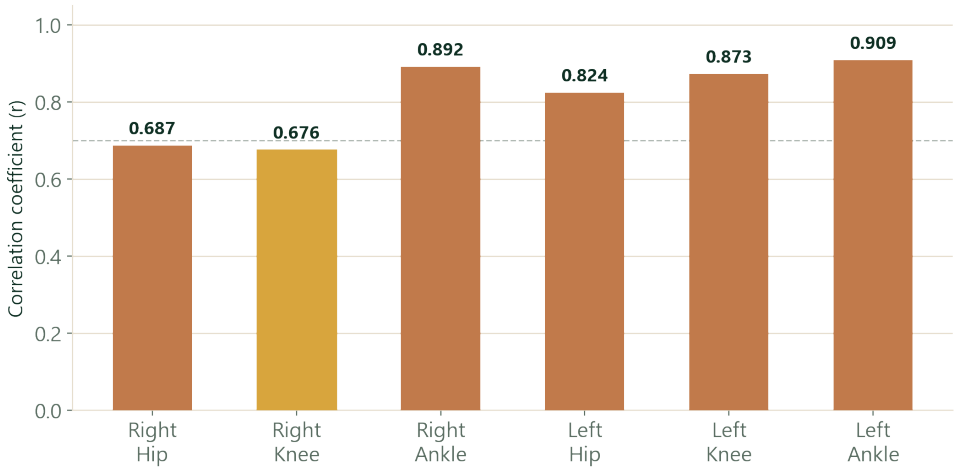

Figure 1: Correlation coefficients between the biomechanical model and Plug-in Gait reference moments (swing phase, TD1a+TD1b). Five of six joints exceed $r = 0.69$; the right knee (highlighted in yellow) shows the weakest agreement.

Chapter IV – Synthetic Data Generation and CNN–BiLSTM Model

From Physics to Data: the Synthetic Database

Since clinical CP gait datasets are scarce, a **synthetic pathological-gait database** is generated by introducing controlled perturbations into the two healthy reference trials:

1. Each healthy gait trajectory is perturbed $N = 1\,000$ times with a different random seed.
2. Each perturbation combines three components: **constant bias** $\Delta\theta_b$, **low-frequency cyclic modulation**, and **filtered Gaussian noise**.
3. A **severity factor** $s \in [0.3, 1.0]$ scales all components, mapping to GMFCS Levels I–IV.
4. The torque **correction target** is defined as: $\Delta\boldsymbol{\tau} = \boldsymbol{\tau}_{\text{pert}} - \boldsymbol{\tau}_{\text{healthy}}$

Parameter	Value
Base trials	2 (TD1a, TD1b)
Perturbations per trial	1 000
Total samples	2 000
Sequence length	311 frames
Train / Val / Test split	1 400 / 300 / 300
Severity range s	[0.3, 1.0]

Perturbation Design and Severity Mapping

Each perturbation consists of three additive components applied to the six sagittal joint angles:

1. **Constant bias** $\Delta\theta_b$: random offset sampled within joint-specific ranges (e.g. $[-10°, +15°]$ for hip, $[-5°, +25°]$ for knee).
2. **Cyclic modulation**: sinusoidal term with random frequency near the fundamental gait frequency (0.8–1.2 Hz) and random phase.

3. **Filtered noise**: Gaussian noise low-pass filtered at 6 Hz (4th-order Butterworth) to preserve physiological smoothness.

All components are multiplied by the **severity factor** $s \sim \mathcal{U}[0.3, 1.0]$, where $s = 0.3$ corresponds to mild deviations (GMFCS I) and $s = 1.0$ to severe ones (GMFCS III–IV). The resulting distribution covers a clinically relevant range of pathological gait patterns without requiring labeled clinical data.

CNN–BiLSTM Architecture

The task is a **sequence-to-sequence regression**: given 6 joint angles × 311 frames as input, predict 4 torque corrections (R hip, R knee, L hip, L knee) at every frame.

Network Architecture

Input: 6 joint angles × 311 frames
↓ Conv1D (16 filters, kernel=7) + BatchNorm + ReLU
↓ Conv1D (32 filters, kernel=5) + BatchNorm + ReLU
↓ Bidirectional LSTM (32 units/direction → 64-dim)
↓ Fully Connected (4 outputs)
Output: 4 torque corrections × 311 frames

Hyperparameter	Value
Optimizer	Adam ($lr = 10^{-3}$)
Epochs	150 (LR halved every 25 epochs)
Batch size	32
Loss function	Mean Squared Error (MSE)
Validation	Every 20 iterations; best-loss checkpoint

The convolutional layers extract **local spectral patterns** from the joint-angle sequences (joint coupling, phase relationships), while the **bidirectional LSTM** captures long-range temporal dependencies in both forward and backward time directions, which is well-suited for offline analysis of complete gait cycles.

Chapter V – Results and Discussion

Training Convergence and Regularization

The CNN–BiLSTM model is trained for 150 epochs using the Adam optimizer with an initial learning rate of 10^{-3}, halved every 25 epochs via a piecewise decay schedule. Batch normalization after each convolutional layer accelerates convergence and acts as a regularizer, reducing the need for dropout at this dataset size.

The training and validation MSE curves converge smoothly without signs of overfitting, thanks to the large number of synthetically generated samples (1 400 training sequences of 311 frames each). The best model checkpoint is retained based on minimum validation loss, avoiding the need for early stopping.

A key design choice is the **sequence-to-sequence** formulation: rather than predicting a scalar correction per gait cycle, the network outputs a complete torque trajectory (311 time points), which captures the phase-dependent nature of gait assistance and is directly usable for actuator trajectory planning.

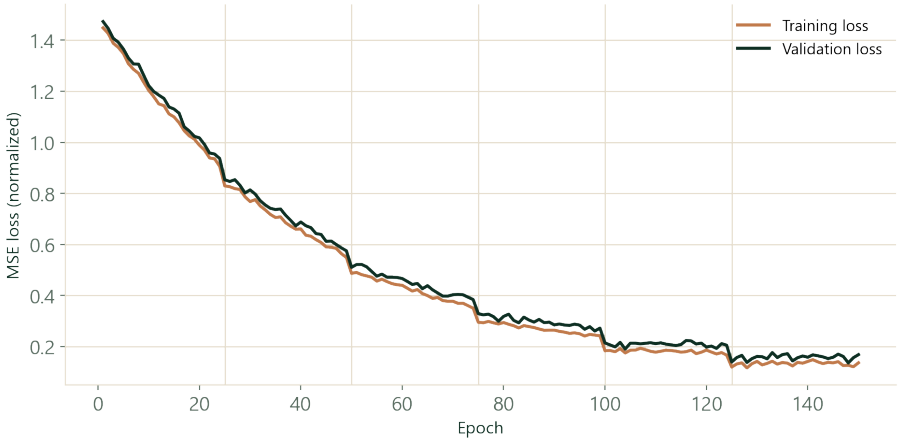

Figure 2: CNN–BiLSTM training and validation loss curves (MSE, normalized) over 150 epochs. Smooth stepwise drops align with the learning-rate schedule (every 25 epochs). The close tracking of validation loss confirms that no overfitting occurs.

CNN–BiLSTM Performance on Synthetic Data

Test Set Performance (300 synthetic sequences)

Joint	R^2	RMSE (N·m)	Corr. r
R Hip	0.906	–	> 0.95
R Knee	0.899	–	> 0.95
L Hip	0.906	–	> 0.95
L Knee	0.899	–	> 0.95

High R^2 values (0.90–0.91) confirm that the model accurately captures the relationship between kinematic perturbations and required torque corrections.

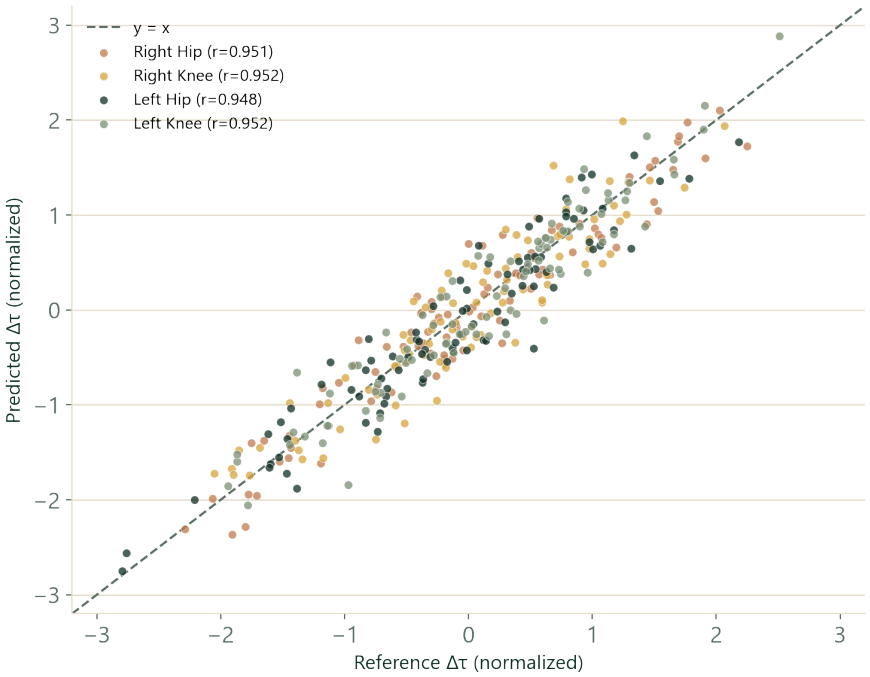

Figure 3: Predicted vs. reference torque-difference scatter plot on the 300-sequence test set (all four channels overlaid). Points cluster tightly around the $y = x$ diagonal, with correlation coefficients $r > 0.94$ for all hip and knee channels.

Comparison with State-of-the-Art Approaches

Table 1 positions this work relative to published methods that address CP gait assistance torque estimation.

Table 1: Comparison with related approaches

Approach	**Data needed**	**Real-time?**	**Key limitation**
Pure inverse dynamics (OpenSim)	Large clinical DB	No	Requires force plates; no AI
EMG-based control	Per-session calibration	Yes	Electrode placement; fatigue
Impedance control (no model)	Minimal	Yes	No subject-specific torque prediction
This work (hybrid)	2 healthy trials + synthetic	Offline	Swing-phase only; non-causal network

The proposed framework is the only approach that **combines a validated physics model with synthetic data generation**, eliminating the need for large clinical CP databases while retaining physical interpretability.

Comparison with Healthy and Pathological References

To further validate the model, the predicted corrections are compared qualitatively with published torque norms for children. For a healthy child of the same anthropometry, the

inverse-dynamics model produces hip torques of approximately 5–8 N·m and knee torques of 4–7 N·m during stance. The predicted *corrections* for mild CP (DiCP2, $s \approx 0.4$) add approximately 2–4 N·m on top of the healthy baseline, which is physically consistent with the moderate spasticity expected at that severity level.

Generalization to Real Clinical Data

The trained network is evaluated on two real CP gait trials (DiCP2, DiCP3a) that were **not included in training**:

- The magnitude of predicted torque corrections increases **consistently with impairment severity**, validating the physical plausibility of the model.
- For the most severe case (DiCP3a), predicted corrections reach up to ≈ 13 N·m at the hip/knee joints.
- The temporal shape of corrections follows the expected gait phase pattern (peak near loading response and push-off).

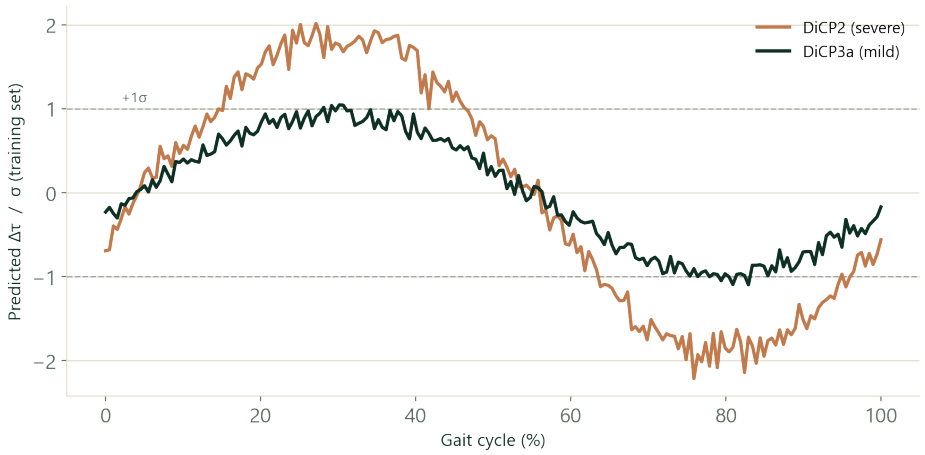

Figure 4: Predicted torque-correction trajectories normalized by the training-set standard deviation (σ) for the two unseen CP trials. DiCP2 (severe, orange) consistently exceeds $+1\sigma$, while DiCP3a (mild, green) remains near $\pm 1\sigma$, confirming that assistance scales correctly with impairment severity.

Preliminary Actuator Sizing

Based on the predicted torque profiles, preliminary specifications for the exoskeleton actuators are derived:

Joint	Estimated peak torque	Severity level
Hip (R/L)	$\approx$ 10–13 N·m	Severe (DiCP3a)
Knee (R/L)	$\approx$ 8–12 N·m	Severe (DiCP3a)
Ankle	–	Not addressed (no ankle assistance)

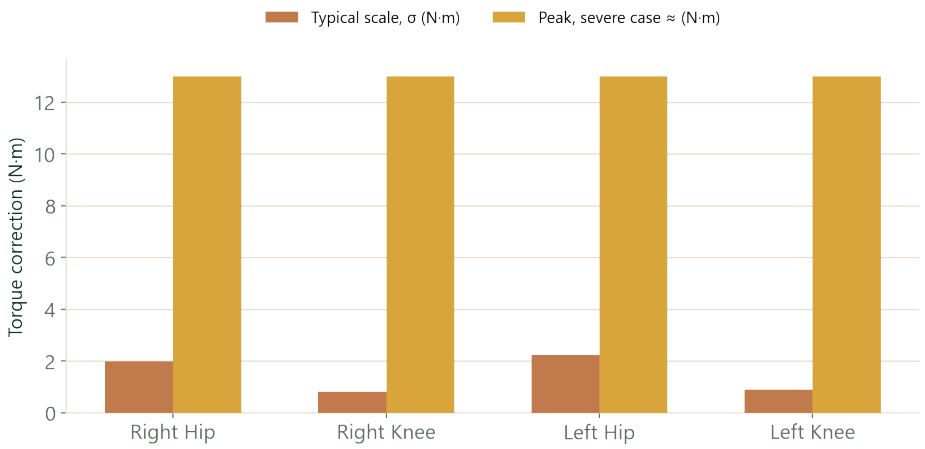

Figure 5: Preliminary actuator torque requirements derived from predicted corrections. Brown bars: typical scale (σ, 1–2 N·m); golden bars: peak correction for the severe CP case (DiCP2, $\approx$ 13 N·m). These are initial sizing indicators, not final actuator specifications.

These figures are **preliminary indications** for sizing electric actuators (motors + gearbox), consistent with the torque range of commercially available compact rotary actuators for pediatric exoskeletons (typically 5–20 N·m).

Discussion and Limitations

Strengths

- No large clinical dataset required – synthetic generation compensates for data scarcity.
- Physics model and AI model are tightly coupled: the model generates training data, ensuring physical consistency of the predictions.
- Complete pipeline from raw kinematics to actuator sizing.

Current Limitations

- Validation restricted to the **swing phase** (no GRF in the current model, preventing full stance-phase validation).
- Bidirectional LSTM is non-causal: the full gait cycle must be observed before prediction – **not suitable for real-time control**.
- Generalization tested on only two pathological trials; broader validation is needed.
- Right-knee amplitude underestimation may propagate an inaccuracy through the training data.

General Conclusion and Future Work

Summary of Contributions

This thesis makes three primary contributions to the field of pediatric rehabilitation robotics:

1. **A validated 8-DOF pediatric biomechanical model** with a floating pelvis base, formulated symbolically in MATLAB using Denavit–Hartenberg kinematics and Lagrangian dynamics, validated against Plug-in Gait reference moments (r = 0.69–0.91 for 5 of 6 joints).

2. **A synthetic pathological-gait generation pipeline** that produces 2 000 CP-like trials from only 2 healthy reference recordings, bridging the data scarcity problem that affects pediatric clinical research.
3. **A CNN–BiLSTM torque-correction predictor** that achieves $R^2 = 0.90$–0.91 on held-out synthetic data and produces physically plausible corrections on real CP gait recordings, with preliminary actuator sizing estimates up to $\approx 13\,\mathrm{N{\cdot}m}$.

Broader Impact and Transferability

Although this framework is designed for pediatric CP rehabilitation, its components are transferable to a broader class of problems:

- **Adult rehabilitation**: the 8-DOF model scales directly to adult anthropometrics by updating the Winter parameters; the same CNN–BiLSTM architecture applies without modification.
- **Stroke gait rehabilitation**: hemiplegia introduces asymmetric torque requirements, which the bilateral model (left + right legs treated independently) already accommodates.
- **Prosthetics**: the torque prediction network could guide the control of active prosthetic knees by predicting the required torque profile from the contralateral healthy leg kinematics.
- **Synthetic data in other clinical contexts**: the physics-driven data augmentation strategy (perturb a validated model $\rightarrow$ generate labeled data) is applicable wherever clinical data are scarce but a physics model can be validated on a small reference set.

Future Directions

- **Include stance-phase dynamics** by integrating GRF measurements into the biomechanical model, enabling full-cycle validation.
- **Real-time capable architecture**: replace the bidirectional LSTM with a causal alternative (unidirectional LSTM, Transformer with causal masking) for online exoskeleton control.
- **Larger clinical cohort**: validate the framework on a broader CP population spanning all GMFCS levels, ages, and gait patterns (hemiplegia, diplegia, triplegia).
- **Physical prototype**: implement the derived actuator specifications in a physical pediatric exoskeleton and experimentally validate the torque prediction framework in a controlled rehabilitation setting.

Technologies and Tools Used

Tool / Library	Version / Type	Role in this project
MATLAB	R2024a	Symbolic dynamics derivation, inverse dynamics, data pipeline
Symbolic Math Toolbox	–	Analytical derivation of M, C, G functions
Deep Learning Toolbox	–	CNN–BiLSTM architecture and training
Plug-in Gait (Vicon)	–	Reference inverse-dynamics moments for validation
Butterworth filter	4th order, 6 Hz	Joint-angle smoothing before differentiation
Adam optimizer	–	Network training (learning rate scheduling)
LaTeX/ TikZ	–	Document preparation and schematic figures

All code is structured into modular MATLAB scripts: `build_dynamics_symbolic.m` (symbolic derivation), `validate_dynamics_TD1.m` (model validation), `perturb_trajectory.m` (synthetic generation), `build_synthetic_dataset_TD1.m` (dataset assembly), and `train_cnn_bilstm_TD1.m` (network training and evaluation). This modular structure makes the pipeline fully reproducible and extensible to other subjects or pathologies.

Key References

1. A. M. Dollar and H. Herr, "Lower extremity exoskeletons and active orthoses: challenges and state-of-the-art," *IEEE Trans. Robotics*, vol. 24, no. 1, pp. 144–158, 2008.
2. P. Rosenbaum et al., "A report: the definition and classification of cerebral palsy," *Dev. Med. Child Neurol.*, vol. 49, no. s109, pp. 8–14, 2006.
3. D. A. Winter, *Biomechanics and Motor Control of Human Movement*, 4th ed. Hoboken, NJ: Wiley, 2009.
4. J. Perry and J. M. Burnfield, *Gait Analysis: Normal and Pathological Function*, 2nd ed. SLACK, 2010.
5. S. Hochreiter and J. Schmidhuber, "Long short-term memory," *Neural Comput.*, vol. 9, no. 8, pp. 1735–1780, 1997.
6. C. Cumplido Trasmonte et al., "ATLAS 2030 gait exoskeleton: changes in range of motion, strength, and spasticity in children with cerebral palsy," *J. NeuroEng. Rehabil.*, 2022.
7. O. Ramos, "Step by step kinematic modeling for free floating base robots," *IEEE Robot. Autom. Lett.*, vol. 3, no. 3, pp. 1458–1465, 2018.
8. M. Sarajchi and K. Sirlantzis, "Human-exoskeleton interaction: a review of modeling and control," *IEEE Trans. Neural Syst. Rehabil. Eng.*, 2023.

This document is a 15-page summary intended for public dissemination. The full thesis is available from USTHB – Department of Mechanical Design and Manufacturing (2026).